European Journal of Pharmacology 902 (2021) 174091

Contents lists available at ScienceDirect

European Journal of Pharmacology

journal homepage: www.elsevier.com/locate/ejphar

Full length article

Mechanistic evaluation of a novel cyclohexenone derivative's functionality against nociception and inflammation: An in-vitro, in-vivo and in-silico approach

Jawad Khan [a], Gowhar Ali [a,*], Umer Rashid [b], Rasool Khan [c], Muhammad Saeed Jan [d], Rahim Ullah [a], Sajjad Ahmad [e], Sumra Wajid Abbasi [f], Atif Ali Khan Khalil [f], RobertD.E. Sewell [g]

[a] Department of Pharmacy, University of Peshawar, Peshawar, 25120, Pakistan
[b] Department of Chemistry, COMSATS University Islamabad, Abbottabad Campus, Pakistan
[c] Institute of Chemical Sciences, University of Peshawar, 25120, Pakistan
[d] Department of Pharmacy, Faculty of Biological Sciences, University of Malakand, Chakdara, 18000 Dir (L), Pakistan
[e] Department of Health and Biological Sciences, Abasyn University, Peshawar, 25000, Pakistan
[f] Department of Biological Sciences, National University of Medical Sciences, Rawalpindi, 46000, Pakistan
[g] School of Pharmacy and Pharmaceutical Sciences, Cardiff University, Cardiff, CF10 3NB, UK. UK

ARTICLE INFO

Keywords:
Cyclohexenone
Anti-nociceptive
Anti-inflammatory
Cyclooxygenase-2
5-Lipoxygenase
$GABA_A$/Opioid receptors

ABSTRACT

The synthesis of a novel cyclohexanone derivative (CHD; Ethyl 6-(4-metohxyphenyl)-2-oxo-4-phenylcyclohexe-3-enecarboxylate) was described and the subsequent aim was to perform an *in vitro*, *in vivo* and *in silico* pharmacological evaluation as a putative anti-nociceptive and anti-inflammatory agent in mice. Initial *in vitro* studies revealed that CHD inhibited both cyclooxygenase-2 (COX-2) and 5-lipoxygenase (5-LOX) enzymes and it also reduced mRNA expression of COX-2 and the pro-inflammatory cytokines TNF-α and IL-1β. It was then shown that CHD dose dependently inhibited chemically induced tonic nociception in the abdominal constriction assay and also phasic thermal nociception (i.e. anti-nociception) in the hot plate and tail immersion tests in comparison with aspirin and tramadol respectively. The thermal test outcomes indicated a possible moderate centrally mediated anti-nociception which, in the case of the hot plate test, was pentylenetetrazole (PTZ) and naloxone reversible, implicating GABAergic and opioidergic mechanisms. CHD was also effective against both the neurogenic and inflammatory mediator phases induced in the formalin test and it also disclosed anti-inflammatory activity against the phlogistic agents, carrageenan, serotonin, histamine and xylene compared with standard drugs in edema volume tests. *In silico* studies indicated that CHD possessed preferential affinity for $GABA_A$, opioid and COX-2 target sites and this was supported by molecular dynamic simulations where computation of free energy of binding also favored the formation of stable complexes with these sites. These findings suggest that CHD has prospective anti-nociceptive and anti-inflammatory properties, probably mediated through GABAergic and opioidergic interactions supplemented by COX-2 and 5-LOX enzyme inhibition in addition to reducing pro-inflammatory cytokine expression. CHD may therefore possess potentially beneficial therapeutic effectiveness in the management of inflammation and pain.

1. Introduction

The process of drug discovery and development incorporating a novel chemical moiety with a desirable therapeutic profile is a challenging task nowadays (DiMasi et al., 2010). Extensive research has been carried out on pain and inflammation over a number of years, particularly because these pathological conditions can greatly influence patient quality of life (Ali et al., 2015; Chapman and Gavrin, 1999; Shahid et al., 2017a, 2017b). Pathologically, pain may be categorized as nociceptive, neuropathic or inflammatory and if protracted, it may progress into a chronic pain syndrome involving additional symptoms such as anxiety and depression. Nociceptive pain is typically initiated by stimulation of somatic sensory receptors designated as nociceptors, which then transmit pain impulses to the central nervous system (CNS).

* Corresponding author. Department of Pharmacy University of Peshawar, Peshawar, 25120, KP, Pakistan.
E-mail addresses: gowhar_ali@uop.edu.pk, gohar.pharmacist@gmail.com (G. Ali).

https://doi.org/10.1016/j.ejphar.2021.174091
Received 31 October 2020; Received in revised form 25 March 2021; Accepted 31 March 2021
Available online 16 April 2021
0014-2999/© 2021 Elsevier B.V. All rights reserved.

Alternatively, neuropathic pain arises from damage or lesions to the nervous system (Van Hecke et al., 2014). Active inflammation is the hallmark of inflammatory pain and is characterized by the presence of inflammatory mediators such as interleukin, TNF-α, prostaglandins (PGE2, PGI2, TXA2), histamine, serotonin, bradykinin and leukotrienes (LTs) (Fernandes et al., 2015). These biochemical substances produce changes in neuronal sensitivity and invoke the onset of tissue hypersensitivity associated with inflammation (Kidd and Urban, 2001). Currently, opioids and non-steroidal anti-inflammatory drugs (NSAIDs) are the analgesic agents of choice often utilized in the management of inflammatory pain. However, it is well documented that persistent use of NSAIDs may well cause deleterious effects such as ulceration, hemorrhage or even perforation in the gastrointestinal tract, cardiovascular system disorders and kidney damage (Gutthann et al., 1996; Jones et al., 2008). Similarly, opioid analgesics are considered highly effective as analgesics, but they are associated with dependence liability and other side effects which may limit their usefulness (Laxmaiah Manchikanti et al., 2010; Mayer et al., 1995; Shahid et al., 2016). Consequently, there is a genuine need for substitute drugs that retain the analgesic and anti-inflammatory effectiveness of conventional analgesic agents without their untoward effects (Fawad et al., 2018; Islam et al., 2017, 2019).

The key role of the cyclohexenone ring is well established in the field of biomedical research. It has been documented that this functionality is an integral part of several interesting compounds and is of considerable significance for the development of potentially valuable drugs (Das and Manna, 2015; Fang et al., 2012). Chemically, the cyclohexenone nucleus, serves as a convenient intermediate for synthesizing various heterocyclic compounds including fused pyrazoles, isoxazoles, quinazolines (Senguttuvan and Nagarajan, 2010) and 2H-indazole (Gopalakrishnan et al., 2008). Cyclohexenones are cyclohexane derivatives with a carbonyl group at position-1 and a carbon-carbon double bond at position-2 (Fig. 1). The enone functional group and substitution at a carbon atom in the six membered ring have been used to synthesize other substituted cyclohexenones (Johnson et al., 2016). The pharmacological properties of cyclohexenone derivatives include anti-inflammatory and anti-nociceptive effects (Ahmadi et al., 2012; Lednicer et al., 1981a, 1981b; Liu et al., 2013; Ming-Tatt et al., 2012, 2013; Sheorey et al., 2016; Wang et al., 2011) as well as anti-neuropathic and antioxidant activity (Khan et al., 2019). The present study was undertaken to evaluate a novel cyclohexenone derivative (CHD; Ethyl 6-(4-metohxyphenyl)-2-oxo-4-phenylcyclohexe-3-enecarboxylate) as a possible inhibitor of cyclooxygenase-2 (COX-2) and 5-LOX pro-inflammatory enzymes and subsequently examine its effects against nociception using *in vivo* mouse models of pain and inflammation. Additionally, the anti-nociceptive activity of CHD was also investigated in the presence of pentylenetetrazole (PTZ) and naloxone in order to probe any possible underlying mechanisms, which might have been corroborated by *in silico* and *in vitro* studies.

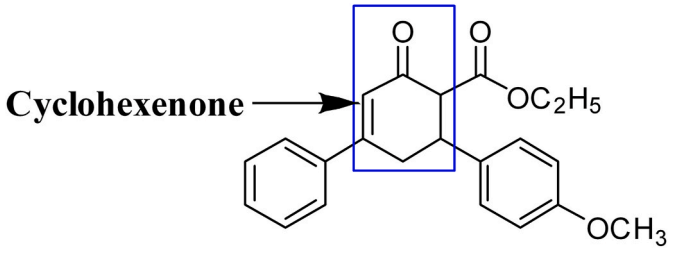

Fig. 1. Chemical structure of Ethyl 6-(-4-methoxyphenyl)-2-oxo-4-phenylcyclohex-3-enecarboxylate.

2. Material and methods

2.1. Chemicals and drugs

Naloxone, serotonin, histamine, PTZ, xylene, indomethacin, lambda carrageenan and aspirin were purchased from (Sigma-Aldrich, USA). Formaldehyde was procured from Merck (Germany), glacial acetic acid was obtained from Pancreac (Spain), tramadol (Tramal® 50 mg/ml) was acquired from Searle Ltd (Pakistan). Fresh preparation of chalcone was carried out in the laboratory of ICS (University of Peshawar, Pakistan). Ethyl acetoacetate, ethyl acetate and potassium carbonate were purchased from Merck (Pakistan). N-hexane and ethanol were procured from Scharlau (Lahore, Pakistan). The cDNA synthesis kit, TRIzol reagent, master mix and primers were acquired from Thermofishcer Scientific (USA).

2.2. Chemistry

2.2.1. General

A Gallenkamp melting point apparatus was used to determine melting points. Purity was checked by thin layer chromatography (TLC). A Shimadzu IR Prestige-21 FT-IR Spectrometer Instrument (Tokyo, Japan) was utilized to record the Infrared spectra. ^{13}C and ^{1}H NMR analyses (Agilent AV-300,400 and 500 Tokyo, Japan) were accomplished with D_2O and DMSO-d_6 as solvents. Mass spectra (ESI-MS) were obtained on (Qp 2010 plus, Shimadzu, Tokyo, Japan). PerkinElmer 2400 CHN/O Analyzer was operated to determine Elemental analysis.

2.2.2. Synthesis of ethyl 6-(4-metohxyphenyl)-2-oxo-4-phenylcyclohexe-3-enecarboxylate

The synthesis was conducted according to the synthetic protocol as shown in Scheme 1. (E)-3-(-4-methoxyphenyl)-1-phenylprop-2-en-1-one (10 mmol) was refluxed with ethyl acetoacetate (20 mmol) in the presence of K_2CO_3 catalyst in 20 ml of ethanol for 3 h. The product obtained was recrystallized from ethanol; a brownish yellow powder was obtained having a yield of 85%. M.p = 92-95 ^{0}C; Rf = 0.51 *n*-Hexane/ethyl acetate (7:3); IR (KBr) υmax cm-1: 3077 (Ar–H), 1689 (ketone C═O), 1735 (Ester C═O) 2870 (Aliphatic C-H); ^{1}H-NMR ($CDCl_3$, 400 MHz) δ:6.9–7.5 (m, Ar–H),3.05 (d, 2H, J = 2.3), 2.9 (t,1H J = 5.0, C-3), 2.6–2.8 (q, 5H, CH_2CH_3, J = 7.0); ^{13}C-NMR (100 MHz, $CDCl_3$) δ: 199.0 (C═O), 125-130 (Ar-CH), 112 (C-6), 40.2 (OCH_3), 159.0 (C-19), and 44.39 (C-3). EI-MS; m/z (rel. int. %) 351 (M+), CHN Anal. Calcd for: C, 75.41; H, 6.33; O, 18.26. Found: C, 74.81; H, 6.38. Formula: $C_{22}H_{22}O_4$, C = 22, H = 22, and O = 4.

2.3. In vitro activities

2.3.1. 5-LOX inhibition assay

The inhibitory potential of CHD was examined by utilizing human recombinant 5-LOX. In this assessment, the enzyme inhibition was determined through residual enzyme potential following 10 to 15 min incubation at 25 °C in an incubator (Jan et al., 2020; Wisastra et al., 2013). The activity was estimated through linoleic acid (lipoxygenase substrate) conversion into hydroperoxy-octadecadienoate (HPOD). The alteration rate was calculated in the form of absorbance at 234 nm with UV–visible spectrophotometer. Ethylene diamine tetra acetic acid (EDTA 2 mM) and $CaCl_2$ (2 mM) containing Tris buffer (50 mM) of PH 7.5 was used as an assay buffer for this assay. The enzyme 5-LOX (20,

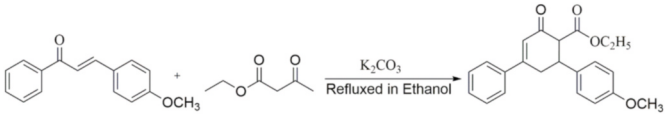

Scheme 1. Synthetic scheme of Ethyl 6-(4-metohxyphenyl)-2-oxo-4-phenylcyclohexe-3-enecarboxylate.

000 U/ml) was diluted with buffer in a ratio of 1:4000. The assay buffer was then diluted with 100 mM of inhibitor formerly blended with DMSO. Linoleic acid was then diluted with ethyl alcohol to 20 mM. Subsequently, various concentrations of CHD ranging from 31.25 to 1000 μg/ml and 1 ml of enzyme solution (1:4000) was mixed with 100 μl adenosine triphosphate (2 mM), 790 μl of Tris buffer plus 100 μl inhibitor (1 mM) and then incubated for 10 min duration. Then to this mixture was added 10 μl of substrate solution (20 mM) and after 10 s mixing of the enzyme with substrate, the substrate conversion rate was monitored. The reaction rate in the absence of inhibitor was employed as positive control. The standard inhibitor agent used in this assay was zileuton.

2.3.2. COX-2 inhibition assay

The COX-2 inhibitory activity of the test compound was evaluated according to a previously validated procedure (Burnett et al., 2007; Jan et al., 2020). A COX-2 enzyme solution (300 U/ml) was prepared. For activation, 10 μl of enzyme solution was kept for 5 to 6 min on ice (4 °C) and then mixed with 50 μl of co-factor solution comprising 0.9 mM glutathione, 1 mM hematin in 0.1 mM Tris buffer (pH 8.0) and 0.24 mM tetramethyl-p-phenylenediaminedihydrochloride (TMPD). Then various concentrations (31.25 to 1000 μg/ml) of test sample (20 μl) plus enzyme solution (60 μl) were maintained at room temperature for 5 to 10 min, followed by initiation of the reaction by adding 30 mM arachidonic acid (20 μl) and keeping this mixture at 37 °C for a duration of 15 min. Afterwards, the reaction was terminated by addition of hydrochloric acid (HCL) and absorbance was measured via a UV–visible spectrophotometer at 570 nm. COX-2 percentage inhibition was calculated from the absorbance value per unit time. In the study Celecoxib was utilized as the standard inhibitor agent.

2.3.3. Reverse transcription polymerase chain reaction (RT-PCR)

Post-mortem mouse paw sub plantar tissues were removed 5 h after carrageenan administration and RNA was extracted using TRIzol reagent according to the manufacturer's protocol. The total RNA was reverse transcribed to cDNA following a standard protocol. The primers for targeted genes use were;

COX-2: F-5'-GGAGAGACTATCAAGATAGTGATC -3', R- 5'- ATGGTCAGTAGA-CTTT-TACAGCTC-3'. TNF-α: F-5'-CTTCTCCTTCCTGATC GTGG-3'; R-5'-GCTGGTTAT-CTCTCAGCTCCA-3'. IL-1β: F-5'-AGAAGCTTCCACCAATACTC-3', R-5'-AGCACCTAG-TTGTAAGGAAG-3'. GAPDH: F-5'-TGCACCACCAACTGCTTAGC-3'; R- 5'-GGCATG-GACTGTGGTCATGAG3' was used as a housekeeping gene (Cheon et al., 2009; Khalid et al., 2018). Amplified products were separated using 1.5% Agarose gel electrophoresis, analyzed with image J software (Almeer et al., 2019; Ullah et al., 2021).

2.4. In vivo pharmacological evaluation

2.4.1. Animals

Mice (Balb-C) of either sex weighing 18–30 g were used during the investigation unless otherwise stated. Animals were maintained on standard laboratory food and water *ad libitum* at an ambient temperature of 22 ± 2 °C through a thermostatically controlled air conditioning system on a 12/12 h light and dark cycle and they were habituated to laboratory conditions for 2 h before experiments.

2.4.2. Ethical approval

The study and all *in vivo* protocols were conducted under a project entitled "Studies on the nociceptive, inflammatory and neuropathic pain relieving potential of a cyclohexenone derivative." It was approved by the Research Ethical Committee of the Department of Pharmacy, University of Peshawar, Pakistan which issued a certificate number of 01/EC/18/Pharm. Furthermore, animal experiments were performed in compliance with the Animals Scientific Procedure Act UK (1986).

2.4.2. Acute toxicity study of compound CHD

The acute toxicity profile of CHD was evaluated after intraperitoneal (i.p) injection of selected doses (on a sequential dose-doubling increasing scale viz 15, 30, 60, 120 or 240 mg/kg (n = 6)). Animals were observed at 30–60 min and 24–72 h for any abnormal behaviour (Akbar et al., 2016).

2.4.3. Anti-nociceptive activity

2.4.3.1. Anti-nociceptive activity of compound CHD and a standard drug in the acetic acid abdominal constriction test. Food and water were withdrawn 120 min prior to animal experiments. One percent acetic acid (10 ml/kg) i.p injection was used to induce abdominal constriction as a reflection of tonic nociception. Five min after acetic acid i.p injection, the incidence of abdominal constrictions was recorded over a 20 min period (Abbas et al., 2011). The animals were randomly allocated to different investigational groups (n = 6). Group I received normal saline as vehicle, group II-IV received standard aspirin (15–45 mg/kg), group V-VII received test compound (CHD) (15–45 mg/kg) via i.p injection, 30 min prior to 1% acetic acid injection. Percentage analgesia was calculated using the following formula:

% protection = (1- mean number of abdominal constrictions of the treated drug / mean number of abdominal constrictions of the vehicle control) × 100

2.4.3.2. Anti-nociceptive activity of compound CHD compared to a standard drug in the hot plate test. The hot plate analgesiometer, was kept at a constant temperature of 54 ± 0.1^0 C. After placement on the plate, animal nociceptive reaction latencies (s) were determined to the following escape end points: paw licking, flinching or jumping and a 30 s cut off time was imposed after which mice were removed from the stimulus (Ahmad et al., 2017; Rukh et al., 2020). Animals were randomly assigned to groups (n = 6) and administered saline or drug treatment intraperitoneally. Group I received normal saline as vehicle, group II received standard drug (tramadol, 30 mg/kg, i.p), groups III-V received the trial compound (CHD, 15–45 mg/kg, i.p).

2.4.3.3. Pharmacological antagonism study of CHD compared to a standard drug. In order to evaluate the possible involvement of $GABA_A$ or opioid receptors in the anti-nociceptive activity of CHD, mice were administered PTZ (15 mg/kg; i.p) or naloxone (1 mg/kg; subcutaneously (s.c)) 10–20 min prior to i.p dosing with saline, CHD or standard drug. Hot plate latencies were recorded 30,60 and 90 min after administration of each drug (Muhammad et al., 2012). Percentage protection against nociception was determined using the following formula:

% protection = (Test latency– baseline latency)/ (cut off time– baseline latency) × 100

2.4.3.4. Anti-nociceptive activity of CHD compared to a standard drug in the tail immersion test. Each animal was gently held in a vertical position and half of the tail was immersed in a water bath maintained at a temperature of 55 ± 0.5 °C. A nociceptive reaction latency (s) was determined to a tail flick end point and a cut off time of 15 s imposed after which animals were removed from the stimulus. Any non-responders within the cut-off time were excluded from the study. The vehicle, standard tramadol (30 mg/kg) and test compound (15–45 mg/kg) were administered i.p to their respective groups. The readings were taken at 30, 60, 90 and 120 min after drug administration (Sewell and Spencer, 1976).

2.4.3.5. Anti-nociceptive activity of CHD and standard drug in the formalin induced biphasic pain model. Mice were administered a sub plantar

injection of 20 μl of freshly prepared 2% formalin in the right hind paw. Thirty min prior to formalin injection, groups I-VI, received intraperitoneally normal saline as vehicle, standard drugs indomethacin (10 mg/kg) or diclofenac (10 mg/kg), and CHD (15–45 mg/kg). The nociceptive reaction time (s) (latency to biting, licking, paw lifting or flinching) was measured in two phases: first phase (0 to 5 min) and second phase (10–30 min) after the formalin injection (Silva et al., 2017; Maione et al., 2020).

2.4.4. Anti-inflammatory activity

2.4.4.1. Anti-inflammatory activity of compound CHD and standard in a carrageenan induced paw edema model. Mice were treated with normal saline, aspirin (50–150 mg/kg) or test compound (CHD, 15–45 mg/kg, i.p) 30 min before s.c injection of 0.05 ml of freshly constituted carrageenan (1%) in the right hind paw. A digital Plethysmometer was utilized to determine the inflammation in terms of paw edema volume (ml) at hourly intervals up to 5 h post carrageenan injection (Ali et al., 2013).

2.4.4.2. Anti-inflammatory activity of compound CHD and standard drug in a histamine induced paw edema model. Inflammation was induced in mice (25–30 g) by sub plantar injection of 0.1 ml freshly constituted histamine (1 mg/ml) in the right hind paw. Paw inflammation swelling was measured by means of plethysmometer previously described in the carrageenan test (Mequanint et al., 2011).

2.4.4.3. Anti-edema activity of CHD and a standard drug in the serotonin induced paw volume model. Mice were administered serotonin (0.001 mg/ml s.c) into the plantar surface of the right hind paw. The ensuing inflammation and paw edema was measured by plethysmometer (Masresha et al., 2012).

2.4.4.4. Anti-inflammatory action of compound CHD and standard drug in the xylene provoked ear edema model. In mice weighing 25–35 g, ear edema was evoked by topical application of 0.03 ml of xylene to the internal and outer surface of the right ear while the left ear was used as control. Thirty min before induction of xylene edema, saline vehicle was administered i.p to group I, standard indomethacin (10 mg/kg) or diclofenac (15 mg/kg) to groups II-III and test compound CHD (15–45 mg/kg) to groups IV-VI respectively. Subsequently, 15 min after xylene application, animals were killed and the ears were amputated then weighed. The mean weight difference between right and left ears was then determined (Manouze et al., 2017).

2.5. In silico activity

2.5.1. Docking studies

Docking studies were executed through the Molecular Operating Environment (MOE) version 2016.08 docking program. Three-dimensional (3D) structures of the enzymes, $GABA_A$ and opioid receptors with their co-crystalized ligands were obtained from the Protein Data Bank as listed in Table 1. The docking algorithm was validated by re-docking of native ligands as shown in Table 1. The computed root mean square deviation (RMSD) between the experimental and re-docked poses was found within a threshold limit < 2 Å. The 3D structures of the compound were constructed in MOE by utilizing Builder Module. Energy minimization of the ligand, preparation of structures of the downloaded enzymes and active site identification was carried out according to our earlier validated methods (Iftikhar et al., 2017, 2018; Rashid et al., 2016). Assessment of docking outcomes and scrutiny of their surface with graphical demonstrations were accomplished with discovery studio visualizer and MOE (Systemes, 2015).

2.5.2. Molecular dynamic simulation of complexes

Molecular Dynamic (MD) simulations were performed using the same protocol as explained in our previous study (Abbasi et al., 2016). MD simulations facilitate understanding of the binding pattern and determine the stability of selected receptor-CHD docked complexes. Using AMBER 18 software, six different systems were prepared to run MD simulations for 50 ns each (Case et al., 2010). In order to verify the structural variations and convergence of the simulated systems, the CPPTRAJ module of AmberTools18's was used to estimate the RMSDs for all the studied systems.

Table 1
Protein Data Bank (PDB) code numbers, names of their co-crystalized ligands and resolution for the enzymes studied.

Enzyme/ Receptor	PDB code	Co-crystalized ligand	Resolution (Å)
COX-1 enzyme	1EQG	Ibuprofen	2.61
COX-2 enzyme	1CX2	1-Phenylsulfonamide-3-trifluoromethyl-5-parabromophenylpyrazole (SC-558)	3.00
$GABA_A$ receptor	4COF	Benzamidine	2.97
μ-opioid receptor	4DKL	β-Funaltrexamine (μ-opioid receptor antagonist)	2.8
δ-opioid receptor	4EJ4	Naltrindole (δ-opioid receptor antagonist)	3.4
κ-opioid receptor	4DJH	(3R)-7-Hydroxy-N-{(2S)-1-[(3R,4R)-4-(3-hydroxyphenyl)-3,4-dimethylpiperidin-1-yl]-3-methylbutan-2-yc-1,2,3,4-tetrahydroisoquinoline-3-carboxamide (JDC)	2.9

2.6. Binding free energy calculations

The MMPB/GBSA methods, integrated in AMBER 18, were employed to calculate the binding free energies for all six systems (Miller III et al., 2012). Binding free energy calculations were performed on 100 snapshots taken from the MD trajectories as described previously by Abro and Azam, . The binding free energy can be expressed as:

$$\Delta G_{bind} = \Delta G_{complex} - [\ \Delta G_{receptor} + \Delta G_{ligand}]$$

where ΔG is the Gibb's free energy calculated by MMGB/PBSA.

2.7. Statistical analysis

The data were analyzed statistically utilizing Graph Pad Prism Software, version 5, for manifold assessments via one-way analysis of variance (ANOVA) with Post-hoc Dunnett's test. Outcomes were regarded as statistically significant at $P < 0.05$.

3. Results

3.1. In vitro activities

All enzyme suppression results are presented as the mean of triplicate determinations for each concentration studied and an IC_{50} value was extrapolated from the overall inhibitory concentration relationships.

3.1.1. 5-LOX inhibitory activity

The 5-LOX inhibitory activity of CHD was examined at various concentrations ranging from 31.25 to 1000 μg/ml and the compound displayed a potent inhibition of 5-LOX with an extrapolated IC_{50} value of 10. 27 μg/ml as compared to the standard 5-LOX inhibitor drug zileuton (extrapolated $IC_{50} = 5.50$ μg/ml) over the same tested concentration range (Table 2).

3.1.2. COX-2 inhibitory activity

CHD disclosed a potent inhibitory action on the COX-2 enzyme as shown in Table 3. It was also evident from the outcomes that CHD

Table 2
5-LOX enzyme inhibitory activity of CHD in comparison with zileuton as a standard 5-LOX inhibitor drug.

Compound	Conc. (μg/ml)	% 5-LOX inhibition (Mean ± S.E.M)	Extrapolated IC_{50} μg/ml
Cyclohexenone derivative (CHD)	1000	89.44 ± 0.55[b]	10.27
	500	83.17 ± 0.72[c]	
	250	78.30 ± 0.64[c]	
	125	73.34 ± 0.63[c]	
	62.5	68.30 ± 0.64[c]	
	31.25	61.93 ± 1.13[c]	
Zileuton	1000	93.55 ± 0.40	5.50
	500	89.37 ± 1.65	
	250	85.50 ± 0.40	
	125	79.60 ± 0.90	
	62.5	74.17 ± 0.72	
	31.25	70.35 ± 0.45	

Data is represented as mean ± S.E.M; Values were significantly different as compared to the positive control (zileuton); n = 3, b = P < 0.01, c = P < 0.001.

Table 3
COX-2 enzyme inhibitory assay of CHD in comparison with celecoxib as a standard COX-2 inhibitor drug.

Compound	Conc. (μg/ml)	% COX-2 inhibition (Mean ± S.E.M)	Extrapolated IC_{50} μg/ml
Cyclohexenone derivative (CHD)	1000	88.91 ± 1.30[c]	8.94
	500	85.00 ± 0.30[c]	
	250	78.76 ± 0.58[c]	
	125	73.67 ± 0.61[c]	
	62.5	67.74 ± 0.61[c]	
	31.25	63.47 ± 0.56[c]	
Celecoxib	1000	95.20 ± 0.15	4.30
	500	91.17 ± 0.53	
	250	86.98 ± 0.85	
	125	81.20 ± 0.65	
	62.5	77.80 ± 0.37	
	31.25	73.11 ± 1.20	

Data is represented as mean ± S.E.M; Values were significantly different ~~as~~ compared to the positive control (celecoxib); n = 3, c = $P < 0.001$.

possessed valuable COX-2 inhibitory activity in comparison with the standard COX-2 inhibitor drug celecoxib. Thus, the IC_{50} value for CHD was extrapolated as 8.94 μg/ml in contrast to that of celecoxib (IC_{50} = 4.30 μg/ml) (Table 3).

3.1.3. RT- PCR

To further investigate the anti-inflammatory potential of CHD, RT-PCR was utilized to assess the mRNA levels of COX-2 enzyme and the pro-inflammatory cytokines TNF-α and IL-1β in the carrageenan induced paw edema test in mice. The outcomes of this assessment revealed that CHD (45 mg/kg) significantly reduced the mRNA expression of COX-2 ($P<0.001$), while in the case of TNF-α and IL-1β, CHD also produced a reduction ($P<0.01$) compared to the carrageenan treated vehicle group. Aspirin (150 mg/kg) as the standard positive control decreased ($P<0.001$) the expression of COX-2, TNF-α and IL-1β as presented in (Fig. 2).

3.2. In vivo pharmacological activity

3.2.1. Acute toxicity of CHD

After i.p. injection of selected doses of CHD (15–240 mg/kg; $n = 6$), there was no acute toxicity observed in gross animal behaviour, neither was any incidence of mortality recorded up to the highest dose. Thus, the maximum tolerated dose (MTD) which was devoid of unacceptable toxicity for CHD was >240 mg/kg.

3.2.2. CHD attenuation of chemically induced tonic nociceptive behaviour

Injection of acetic acid (1%) was accompanied by a significant rise in the nociceptive response perceived as an onset increase in the incidence of abdominal constriction. The percentage protection against this chemically induced tonic nociception in the group of animals treated with CHD at a lower dose (15 mg/kg) decreased the nociceptive response as evidenced by an increase in the percentage protection (44.66%, $P < 0.05$). Likewise, the mid-range CHD dose (30 mg/kg) also protected against acetic acid evoked abdominal constriction (49.78%, $P< 0.01$). and the higher dose (45 mg/kg) had an even greater anti-nociceptive effect (59.81%) reflecting dose dependent activity relative to the saline treated animals. The aspirin positive control also yielded a dose dependant anti-nociceptive response (15–45 mg/kg) versus the saline controls (Fig. 3).

3.2.3. CHD attenuation of phasic thermal nociception

In the hot plate test, the saline treated animal group displayed a control escape response from the thermal nociceptive stimulus of 7.3%, 7.5% and 7.7% after 30, 60 and 90 min respectively. The lower dose of CHD was ineffective in producing any detectable anti-nociception between 30 and 90 min (19.3%–17.6%). However, CHD at 30 mg/kg did produce an anti-nociceptive effect at 30 min (24.5%) and 60 min (20.8%) but this was not evident after 90 min (19.5%). A greater anti-nociceptive response was noted at the 45 mg/kg dose (27.3%, 24.0% and 20.3% at 30, 60 and 90 min respectively) while the tramadol (30 mg/kg) positive control produced an even bigger response 77.6%, 72.0% and 69.7% at 30, 60 and 90 min respectively (Fig. 4).

3.2.4. CHD attenuation of phasic nociception in the tail immersion test

CHD produced a measurable anti-nociceptive response in the tail immersion test at the 30 mg/kg dose (30 min). However, the 45 mg/kg dose produced a peak response at 60 min which subsided by 120 min. Treatment with the positive tramadol control (30 mg/kg), produced an intense long-acting anti-nociceptive effect which lasted up to 120 min (Fig. 5).

3.2.5. CHD attenuation of the formalin induced biphasic nociceptive response

Administration of formalin in the sub-plantar mouse hind paw initiated a marked nociceptive response as indicated by an increase in the duration of biting, licking, lifting and flinching of the affected paw. This was observed throughout the first phase (0–5 min) and also the second phase (15–30 min) following formalin administration in the saline treated animals. Treatment with CHD (15 mg/kg) only diminished the second phase of formalin induced nociception. Conversely, the 30 mg/kg CHD dose was more effective in that it markedly reduced the formalin nocifensive response in both the second and first phases ($P<0.05$). Similarly, treatment with the higher CHD dose (45 mg/kg) did induce an anti-nociceptive response in the first phase, but a more statistically significant response in the second phase. The indomethacin and diclofenac positive controls both at 10 mg/kg generated comparable anti-nociception to CHD in both phases (Fig. 6).

3.2.6. Opioidergic and GABAergic mediation of CHD anti-nociception

Any possibility of GABAergic or opioidergic mechanisms underlying the anti-nociceptive effect of CHD in the hot-plate test were probed using pentylenetetrazole (PTZ) and naloxone as respective antagonists. Hence, the anti-nociceptive effect of CHD (30 and 40 mg/kg), was significantly antagonized ($P< 0.001$) by naloxone (1 mg/kg) implicating

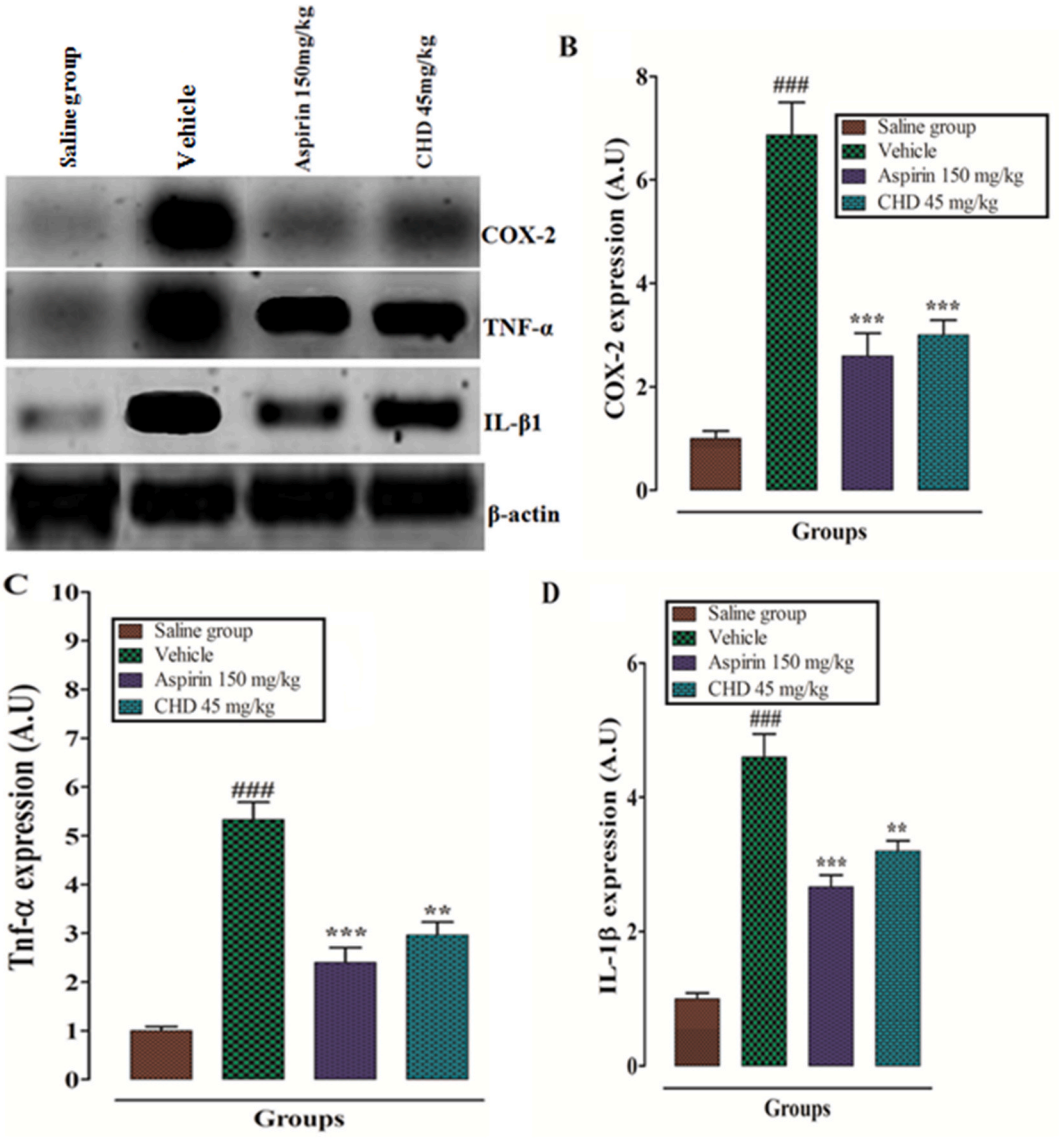

Fig. 2. Agarose gel electrophoresis (A) quantification of CHD activity on the mRNA level of COX-2 (B), TNF-α (C), and IL-1β (D) in carrageenan induced hind paw edema in mice. The results are shown in relative arbitrary units (A.U). Bars represent mean expression in A.U ± S.E.M. $###P < 0.001$ compared to the saline group. $**P< 0.01$, $***P< 0.001$ compared to the vehicle group.

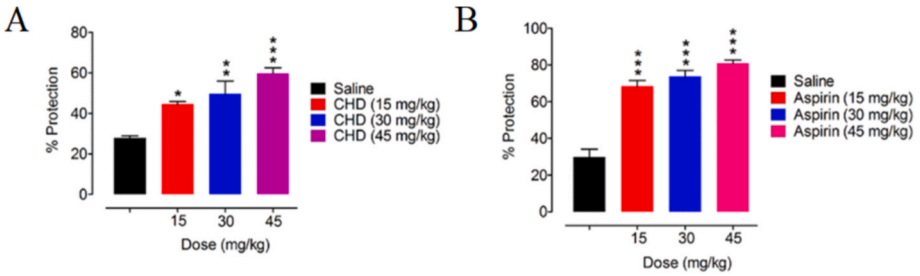

Fig. 3. Anti-nociceptive activity of (A) CHD and (B) the positive control, aspirin in the acetic acid (1%) induced abdominal constriction test. Each bar represents mean percentage protection ±S.E.M). $*P< 0.05$, $**P< 0.01$, $***P< 0.001$ as compared to the saline treated group (one-way ANOVA followed by *post hoc* Dunnett's test), ($n = 6$ mice per group).

the involvement of an opioidergic mechanism. Likewise, in animals treated with the opioid agonist, tramadol (30 mg/kg) as a positive control, naloxone also blocked the anti-nociceptive response (Fig. 7A). Administration of PTZ (15 mg/kg) did not modify the ani-nociceptive action of tramadol (30 mg/kg), but it did markedly decrease the anti-nociceptive response of CHD (30 and 45 mg/kg) in the hot plate paradigm. This would tend to suggest an involvement of a GABAergic mechanism in the anti-nociceptive action of CHD but not tramadol (Fig. 7B).

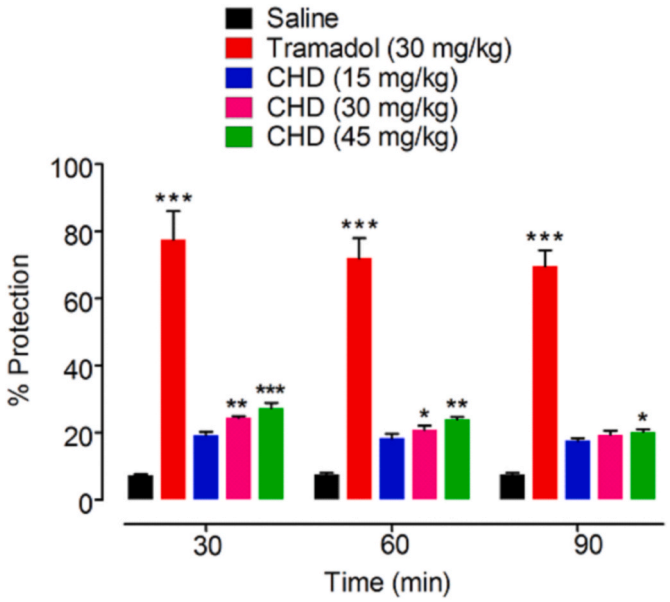

Fig. 4. Anti-nociceptive activity of CHD and the positive control, tramadol, in the hot-plate test. Each bar represents mean percentage protection ±S.E.M). *$P<$ 0.05, **$P<$ 0.01, ***$P<$ 0.001 as compared to saline treated group (one-way ANOVA followed by *post hoc* Dunnett's test), (n = 6 mice per group).

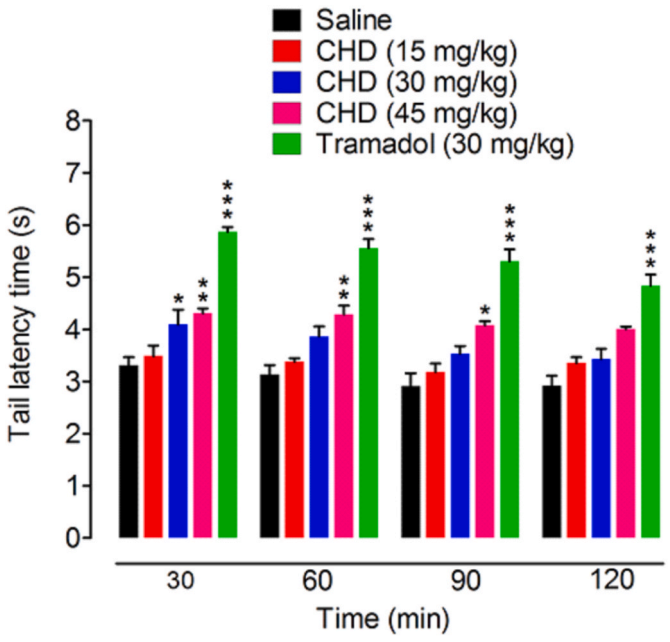

Fig. 5. Anti-nociceptive activity of CHD and the positive control, tramadol in the thermal tail immersion test. Each bar represents mean withdrawal latency time in s ± S.E.M). *$P<$ 0.05, **$P<$ 0.01, ***$P<$ 0.001 as compared to saline treated group (one-way ANOVA followed by *post hoc* Dunnett's test), (n = 6 mice per group).

3.2.7. *Anti-inflammatory action of CHD against phlogistic agents (carrageenan, histamine, and serotonin) in the paw volume inflammation and xylene in the ear inflammation test*

Intraplantar administration of the phlogistic agents, carrageenan, histamine, and serotonin was associated with a pronounced inflammatory response manifested by a substantial increase in the paw volume. The increased edema formation followed a temporal pattern and was first expressed during the initial h of the paradigm and maintained

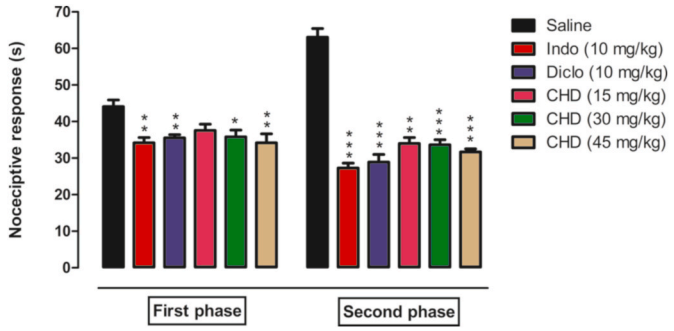

Fig. 6. Anti-nociceptive activity of CHD and the positive controls, indomethacin (Indo), and diclofenac (Diclo) in the formalin induced paw nociceptive test. Each bar represents mean nociceptive response in s ± S.E.M). *$P<$ 0.05, **$P<$ 0.01, ***$P<$ 0.001 as compared to the saline treated group (one-way ANOVA followed by *post hoc* Dunnett's test), (n = 6 mice per group).

throughout the advanced stages of inflammation i.e. up to 5 h of the study duration. A dose dependent anti-inflammatory effect was produced by CHD in the three paradigms of paw edema. Treatment with CHD (15, 30 and 45 mg/kg) reduced the inflammatory response evoked up to 5 h after administration of carrageenan (Fig. 8A), histamine (Fig. 9A), and serotonin (Fig. 10A), Treatment with the aspirin positive control, (50–150 mg/kg) consistently displayed an anti-inflammatory effect up to 5 h after injection of carrageenan, serotonin or histamine in the inflammatory paradigms (Figs. 8B, 9B and 10B).

In the xylene provoked ear inflammatory edema paradigm, application of xylene produced a marked inflammatory response as observed by the increased ear weight recorded in the saline treated control animals (Fig. 11). This marked oedematous change was significantly countered by treatment with CHD (30 and 45 mg/kg). The positive anti-inflammatory control drugs, indomethacin (10 mg/kg) and diclofenac (15 mg/kg) both produced a noteworthy decline in the augmented ear weight edema induced by xylene, as compared to the saline treated controls (Fig. 11).

3.3. *In silico studies*

3.3.1. *Molecular docking*

Docking studies were performed to explore any possible underlying mechanism(s) of CHD anti-nociception and anti-inflammatory activity. Accordingly, simulations were carried out on: (1) cyclooxygenase-2 enzyme (COX-2), (2) GABA receptors and (3) opioid μ-, δ- and κ-receptors using Molecular Operating Environment (MOE 2016.08, Chemical Computing Group, Canada). Data concerning three-dimensional (3D) structures of enzymes with their co-crystalized ligands were downloaded from the Protein Data Bank (PDB) listed in Table 1 and the docking algorithm was validated by re-docking native co-crystalized ligands (Table 1). The computed root mean square deviation (RMSD) between experimental and re-docked poses was found to be within a threshold limit < 2 Å.

The binding orientation of CHD and the native ligand into the binding site of the COX-2 isoform is shown in Fig. 12A. The three-dimensional (3-D) interaction plot of CHD showed that the methoxy group formed a hydrogen bond interaction with His90, an important residue of a selectivity pocket. The carbonyl oxygen formed hydrogen bond interactions with Ala527 (Fig. 12B). The computed binding energy for the CHD-COX-2 complex was −8.1050 kcal/mol and the docking score was −12.0458.

For the GABA receptor, the docking study was carried out on PDB code 4COF (benzamidine). The computed binding energy for the ligand-$GABA_A$ complex was obtained as −5.4853 kcal/mol with a docking score of −8.4314. The superimposed three-dimensional ribbon model of the CHD, (purple), methaqualone (orange) (a positive allosteric $GABA_A$

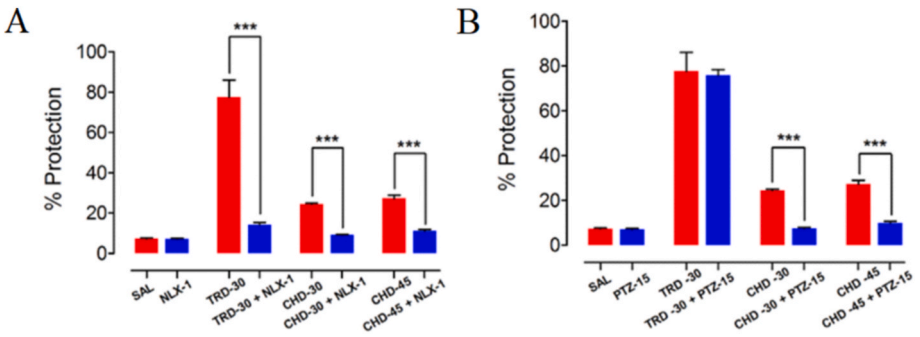

Fig. 7. (A) Effect of naloxone at 1 mg/kg (NLX-1) and (B) PTZ at 15 mg/kg (PTZ-15) on the anti-nociceptive activity of CHD (30 mg/kg, CHD-30 and 45 mg/kg, CHD-45) or tramadol (30 mg/kg, TRD-30) in the mouse hot-plate test. Each bar represents mean percentage protection ± S.E.M. ***P ‹ 0.001 compared to saline control (SAL). (two sample t-test), (n = 6 mice per group).

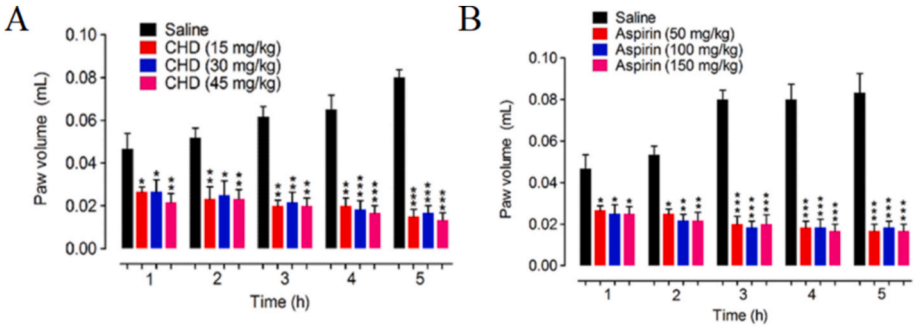

Fig. 8. Anti-inflammatory activity of (A) CHD and (B) the positive control, aspirin in the carrageenan induced paw edema test. Each bar represents paw volume in ml ± S.E.M. *P< 0.05, **P< 0.01, ***P< 0.001 as compared to saline treated group (one-way ANOVA followed by *post hoc* Dunnett's test), (n = 6 mice per group).

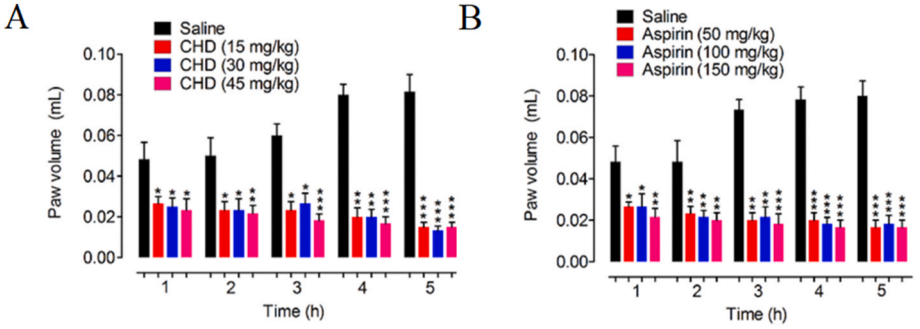

Fig. 9. Anti-inflammatory activity of (A) CHD and (B) the positive control, aspirin in the histamine induced paw edema test. Each bar represents paw volume in ml ± S.E.M. *P< 0.05, **P< 0.01, ***P< 0.001 as compared to saline treated group (one-way ANOVA followed by *post hoc* Dunnett's test), (n = 6 mice per group).

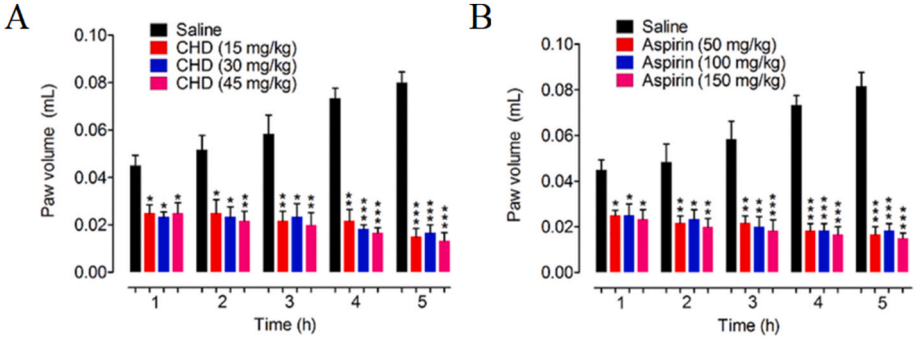

Fig. 10. Anti-inflammatory activity of (A) CHD and (B) the positive control, aspirin in the serotonin induced paw edema test. Each bar represents paw volume in ml ± S.E.M. *P< 0.05, **P< 0.01, ***P< 0.001 as compared to saline treated group (one-way ANOVA followed by *post hoc* Dunnett's test), (n = 6 mice per group).

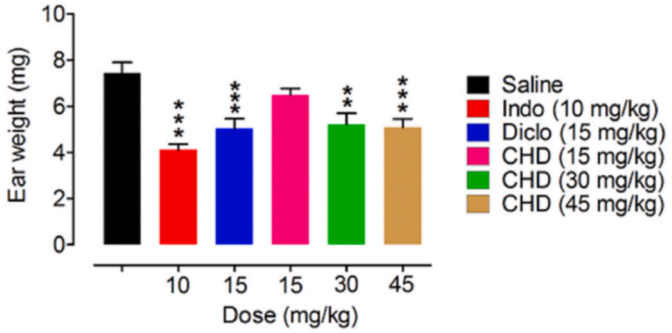

Fig. 11. Anti-inflammatory activity of CHD and the positive controls, indomethacin (Indo), and diclofenac (Diclo) in the xylene induced ear edema test. Each bar represents ear weight in mg ± S.E.M. *$P<$ 0.05, **$P<$ 0.01, ***$P<$ 0.001 compared to the saline treated group (one-way ANOVA followed by *post hoc* Dunnett's test), (n = 6 mice per group).

receptor modulator) and native ligand benzamidine (yellow) is shown in (Fig. 13). The 2D interaction plot showed that the phenyl ring of the synthesized compound creates π-π assembling interactions with Tyr62.

For μ-opioid receptors (μOR), the computed binding affinity for the ligand-receptor complex was −7.0501 kcal/mol and the docking score was computed as −11.4240 (Fig. 14). μOR are important opioid receptors for pain perception and are currently the target of various potent centrally-acting analgesic drugs. The binding pose of CHD (purple) overlaid with β-funaltrexamine is shown in (Fig. 14). The ligand enzyme complex was stabilized by hydrophobic and π-sulfur interactions. The phenyl ring formed π-π stacking interactions with Tyr326, while the 4-methoxyphenyl group formed π-sulfur interactions with Met151.

The binding affinity and docking score in the case of the κ-opioid ligand-receptor complex was calculated as −8.0501 kcal/mol and −12.0240, respectively. The binding pose of the synthesized compound (purple) into the κ-opioid receptor active site (PDB code 4DJH) is shown in Fig. 14. CHD exhibited a binding pose similar to that of the co-crystalized ligand (JDC). The 3D interaction plot showed that the ligand-enzyme complex was stabilized by a hydrogen bond,

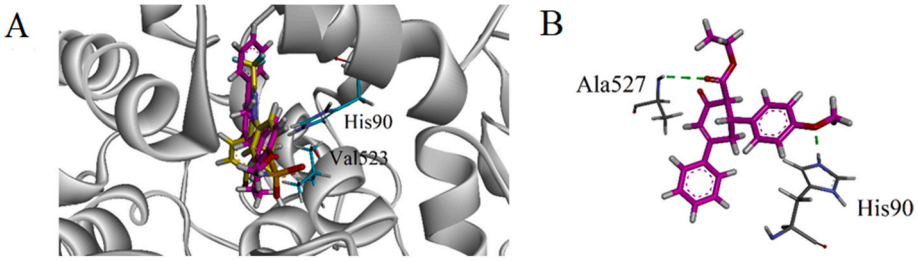

Fig. 12. (A) Ribbon diagram of overlaid binding orientation of CHD and native ligand into the binding site of the COX-2 enzyme. (B) Three-dimensional ligand-enzyme interaction plots of the cyclohexenone derivative (CHD) into the binding site of COX-2 enzyme.

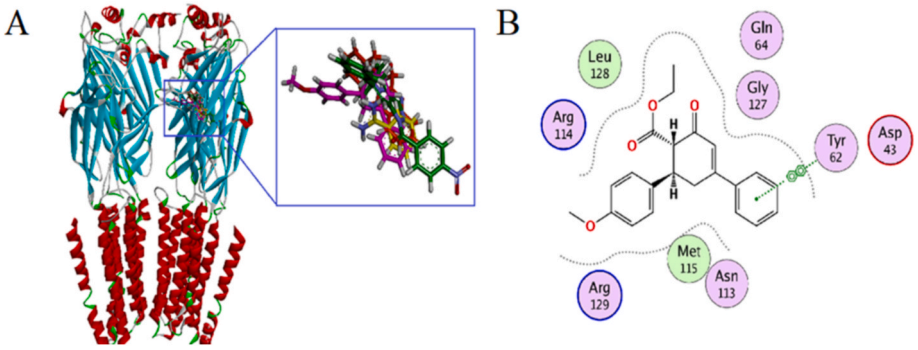

Fig. 13. (A) Three-dimensional superimposed binding pose of the native ligand benzamidine (yellow), cyclohexenone derivative (CHD; purple) and methaqualone (orange) into the binding site of the $GABA_A$ receptor (PDB code 4COF) and (B) Two-dimensional interaction plot for CHD.

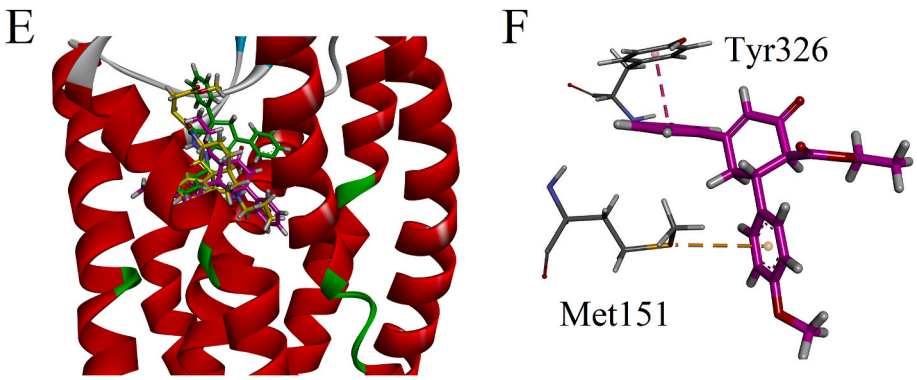

Fig. 14. Three and Two dimensional models of CHD binding with opioid receptors. (A) Three-dimensional and (B) Two-dimensional modeled superimposed binding pose of native ligand and CHD (purple) into the binding site of δ-opioid receptors (PDB code = 4EJ4). (C) Three-dimensional and (D) Two-dimensional model superimposed binding pose of native ligand and CHD (purple) into the binding site of κ-opioid receptor (PDB code = 4DJH). (E) Three-dimensional and (F) Two-dimensional model superimposed binding pose of the native ligand and selected compound CHD (purple) into the binding site of μ-opioid receptors (4DKL).

hydrophobic, π-sulfur as well as π-CH type interactions. Met142 formed π-sulfur interactions with the 4-methoxyphenyl ring. The phenyl ring of CHD engages in π-π stacking interactions with Trp287. A hydrogen bonding interaction was found between the carbonyl oxygen of the ring with Tyr312. Similarly, Val108, Val230, Val290, Ile294 and Ile316 formed some π-alkyl interactions.

For the δ-opioid receptor, the binding affinity for the ligand-enzyme complex was calculated as −7.4000 kcal/mol and the docking score was noted as −11.0903. In the case of δ-opioid receptors, the 3D structure with naltrindole as co-crystalized ligand was retrieved (PDB code = 4EJ4). The superimposed 3D binding pose of CHD (purple) with naltrindole (yellow) is shown in (Fig. 14). The two-dimensional interaction plot showed that it interacted with Met132 *via* hydrogen bond donor interactions.

3.3.2. Molecular dynamics (MD) simulations

MD simulations were performed in order to understand the dynamics of all complexes and check the stability of the CHD conformation at the docked site with respect to the backbone atoms for each receptor. Among the complexes, 4COF, 1CX2, and 1EQG showed good stabilty in the presence of CHD compared to the other three receptors (Fig. 15A).

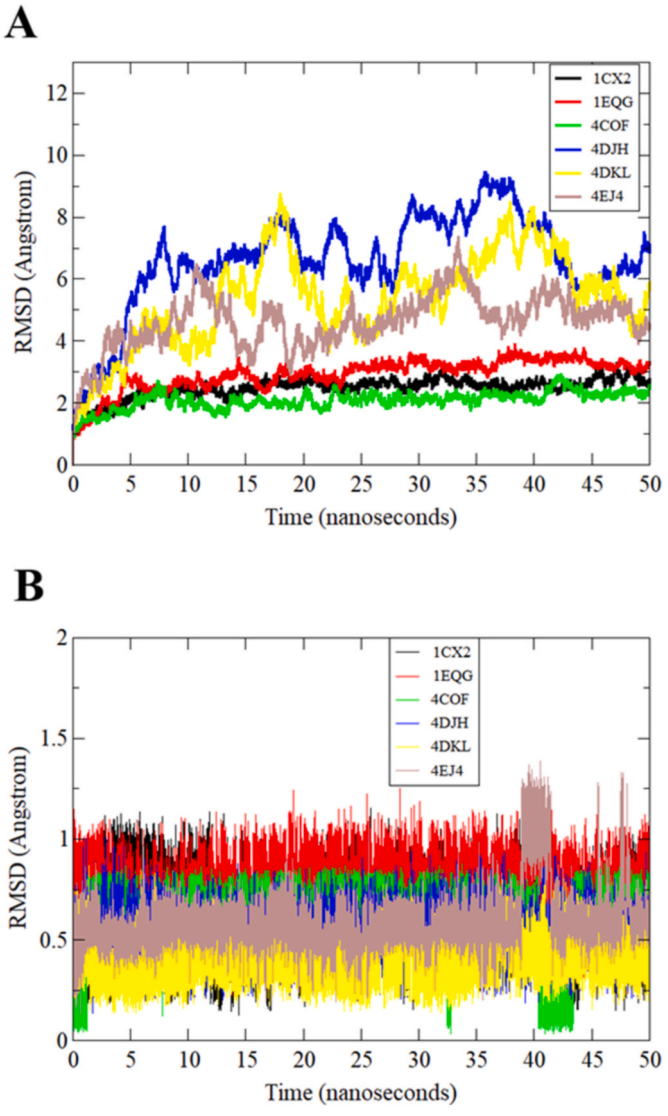

Fig. 15. (A) Root Mean Square Devitaions of backbone atoms for each receptor of docked complexes. (B) CHD Root Mean Square Devitaions over 50-ns of MD simulation in complex with receptors.

The mean RMSDs of these were 2.0 Å, 2.4 Å, and 2.9 Å, respectively. These sites in the presence of CHD at the docked position revealed very constant RMSD patterns throughout the simulaiton time, indicating a good intermolecular strength of affinity and stability pattern. 4DJH (mean RMSD = 6.8 Å), 4DKL (mean RMSD = 5.4 Å), and 4EJ4 (mean RMSD = 4.6 Å) showed major fluctuations in the receptor structures, however, these changes do not affect the binding and conformation of the compound with the receptors. In essence, these RMSD receptor fluctuations correspond to local protein structure movments which are normal to their function. To substantiate compound conformation stability, we additionally computed compound RMSDs in all complexes and plotted them versus time. As can be seen in (Fig. 15B), the compounds were significantly stable with all receptor RMSDs <1 Å in all frames of the MD simulation.

3.3.3. MMPB/GBSA binding energy calculation

The free energy of binding was computed for all complexes to evaluate and revalidate the affinity of intermolecular interactions and discover which type of interaction energy was dominant in contributing to complex stability. All the complexes divulged robust interaction energies and were dominated by gas phase energy in both MMGBSA and MMPBSA methodologies. Solvation energy appeared to play less of a role in molecular interactions and was therefore non-favorable. More specifically, the van der Waals energy of the gas phase disclosed by both methods played a key role in complex stability whereas a minor contribution from electrostatic energy was also evident except in the case of ICX2.The non-polar energy of solvation also favored docked molecules as opposed to a highly unfavorable contribution from polar solvation energy. Overall, the 4DKL receptor in complex with the CHD compound was highly stable with a MMGBSA energy of −55.4492 kcal/mol and −47.9865 kcal/mol in MMPBSA. Details of MMGBSA and MMPBSA energies of the complexes can be viewed in Table 4.

4. Discussion

Cyclohexenone derivatives have received considerable attention over recent years not only preclinically, but also clinically because of their extensive pharmacological possibilities. These include: analgesic (Said et al., 2009), anti-inflammatory (Yaouba et al., 2018), anti-neuropathic (Khan et al., 2019), antipyretic (Mousavi, 2016), antibacterial (Saranya and Ravi, 2012), antioxidant (Okoth et al., 2016), antifungal (Kanagarajan et al., 2013), antimalarial (Ledoux et al., 2017), anti-tubercular (Monga et al., 2014), anti-leishmanial (Das and Manna, 2015), anticonvulsant (Said et al., 2009) tyrosine kinase inhibitory (Nazar et al., 2015) cytotoxic (Ayyad et al., 1998) and anticancer (Okoth and Koorbanally, 2015) activities. Bearing in mind these wide-ranging potential capacities of cyclohexenone functionality, this study was designed to examine a selected cyclohexanone derivative (CHD) exemplar (Ethyl 6-(4-metohxyphenyl)-2-oxo-4-phenylcyclohex-e-3-enecarboxylate). This was done firstly for its safety profile; secondly, to investigate any feasible *in vivo* effects in standard animal models of nociceptive and inflammatory pain; thirdly, to perform molecular docking and molecular dynamic (MD) simulation studies to facilitate interpretation of targeted drug-receptor interactions to corroborate the *in vivo* findings. In parallel with this research approach, *in vitro* assays were conducted to examine any possibility of COX-2 or 5-LOX enzyme inhibition and/or suppression of mRNA expression of TNF-α, IL-1β and COX-2 that might underlie anti-nociceptive and anti-inflammatory effects.

Four nociceptive and inflammatory, highly reproducible standard models were used to generate the results. The findings clearly indicated that CHD possessed a noteworthy degree of safety with a maximum tolerated dose above 240 mg/kg. Statistically significant anti-nociceptive and anti-inflammatory activity was found in the rodent models. These effects were comparable to those of aspirin, tramadol, indomethacin and diclofenac used as positive controls (Figs. 3–11).

Table 4
MGBSA and MMPBSA binding energies of the complexes.

Method	Energy Component	1EQG	1CX2	4COF	4DKL	4EJ4	4DJH
MMGBSA	VDWAALS	−40.4511	−52.1322	−47.2564	−62.2517	−61.1760	−53.3142
	EEL	−6.2952	3.4110	−25.3784	−8.2760	−10.7373	−9.9464
	EGB	18.2375	8.9329	35.5743	21.3416	24.9894	19.8313
	ESURF	−4.3177	−5.6008	−4.8037	−6.2631	−6.2177	−5.5521
	DELTA G gas	−46.7463	−48.7212	−72.6348	−70.5277	−71.9133	−63.2606
	DELTA G solv	13.9198	3.3320	30.7706	15.0785	18.7716	14.2792
	DELTA TOTAL	−32.8265	−45.3892	−41.8641	−55.4492	−53.1417	−48.9814
MMPBSA	VDWAALS	−40.4511	−52.1322	−47.2564	−62.2517	−61.1760	−53.3142
	EEL	−6.2952	3.4110	−25.3784	−8.2760	−10.7373	−9.9464
	EPB	22.4009	14.6505	40.4885	26.2948	32.7712	26.3717
	ENPOLAR	−2.9491	−3.5859	−3.3982	−3.7537	−3.7336	−3.6908
	EDISPER	0.0000	0.0000	0.0000	0.0000	0.0000	0.0000
	DELTA G gas	−46.7463	−48.7212	−72.6348	−70.5277	−71.9133	−63.2606
	DELTA G solv	19.4518	11.0646	37.0904	22.5411	29.0376	22.6810
	DELTA TOTAL	−27.2945	−37.6567	−35.5444	−47.9865	−42.8757	−40.5796

Moreover, *in silico* docking analysis demonstrated that CHD manifested favorable interactions with common pain targets i.e. COX-1/2 enzymes in addition to opioid and $GABA_A$ receptors (Figs. 12–14.) substantiating the in-vivo results. Equally, CHD produced marked inhibition of COX-2 and 5-LOX in the enzyme assays while in the case of RT-PCR, CHD reduced the mRNA expression of TNF-α, IL-1β and COX-2.

Administration of GABA receptor agonists either supraspinally, spinally or peripherally, has been reported to reduce the nociceptive index in models of neuropathic and inflammatory pain (Malan et al., 2002; Patel et al., 2001). In our study, it is postulated that CHD alleviates centrally mediated nociception via GABAergic and opioidergic mechanisms (Fig. 7) alongside a capability of interaction with the COX-1/2 target (Fig. 12). An involvement of GABAergic and opioidergic systems was further reinforced by computational studies whereby CHD exhibited favorable binding affinity for the $GABA_A$ (Fig. 13) and opioid receptor subtypes (μ, κ and δ) (Fig. 14). It has been reported that GABAergic agonists may augment the anti-nociceptive effect of a centrally acting analgesic such as morphine (Sawynok, 1984), hence, it is conceivable that GABA receptor agonist administration may represent a therapeutic option for the management of both chronic and acute pain (McCarson and Enna, 2014) or as a combination of GABA with opioid receptor related therapies.

The acetic acid induced abdominal constriction assay is a tonic visceral pain model frequently utilized for monitoring the anti-nociceptive action of drugs (Utsunomiya et al., 1998). Although it is a very sensitive test, it cannot distinguish whether the nociceptive activity is peripherally or centrally mediated (Chen et al., 1995). It entails stimulation of visceral receptors followed by the release of bradykinin, serotonin, cyclooxygenase, prostaglandins and interleukins which induce pain and inflammation (Olonode et al., 2015; Rodrigues et al., 2012). It also implicates an enhanced activation of peripheral receptors (Bentley et al., 1983) and innervated nociceptive nerve terminals (Duarte et al., 1988). In the current study, CHD induced a significant reduction in abdominal constrictions in a dose-dependent manner comparable to standard aspirin (Fig. 3A and B).

Hot plate and tail immersion nociceptive tests were employed to determine the central anti-nociceptive potential of CHD. These models can specifically evaluate possible central nociception (Eddy and Leimbach, 1953), where there is a non-inflammatory and acute nociceptive reaction developed upon exposure to heat via spinal receptors which is evidence of centrally mediated anti-nociception (Amabeoku and Kabatende, 2012; Pini et al., 1997). CHD moderately enhanced the hot plate latencies of mice compared to standard tramadol, suggesting it to be a centrally acting analgesic (Fig. 4). In the tail immersion test, the behavioural response is predominantly controlled by supraspinal and spinal entities (Danneman et al., 1994). At the doses studied, CHD presented a modest increase in tail withdrawal latency, but tramadol produced a more pronounced latency elevation (Fig. 5). The duration of action of a drug depends on several factors including biological half-life, first pass effect, plasma protein binding and other pharmacokinetic factors, nature of formulation, co-morbid conditions such as renal impairment or liver disfunction. Any of the above cited factors, may be a potential contributor to the loss of CHD effectiveness at the doses of 30 and 45 mg/kg in the thermal nociception tests within 90 min (hot plate test) and 120 min (tail immersion test), respectively. The formalin induced nociceptive paradigm comprises of a binary phased nociceptive reaction and neuropathic pain (Salinas-Abarca et al., 2017). A neurogenic or first phase (0–5 min) in which class C fibres are stimulated and an inflammatory or second phase (10 to 30 min) which involves the release of inflammatory mediators (Hunskaar and Hole, 1987; Tjølsen et al., 1992). Interestingly, CHD was effective in both the neurogenic and inflammatory mediator phases (Fig. 6), further reinforcing the concept of a possible centrally acting anti-nociceptive component mechanism in the activity of this compound. Moreover, in experiments involving pharmacological antagonism of CHD anti-nociception with PTZ and naloxone, it was divulged that an apparent participation of both GABAergic and opioidergic mechanisms was implicated (Fig. 7A and B).

The anti-inflammatory activity of CHD was investigated by employing four standard models of inflammation i.e., the carrageenan, serotonin, histamine and xylene mediated edema tests (Figs. 8–11). The carrageenan incited paw volume model is most extensively employed for evaluating the anti-edematous potential of drugs (Mazzanti and Braghiroli, 1994). Localised paw injection of carrageenan in mice initiates a three-phased inflammatory process. The primary phase (0 to 1.5 h), is caused by the release of serotonin and histamine whereas the secondary phase (1.5 to 2.5 h) is mediated via bradykinin and the tertiary phase (2.5 to 5 h) is elicited mainly by the generation of prostaglandins (Suba et al., 2005).

CHD (15–45 mg/kg) substantially reduced the elevated paw edema in all three phases of the carrageenan-induced paw volume assay and this was comparable to the response yielded by the standard drug, aspirin (Fig. 8A and B). In order to authenticate the finding from the carrageenan paw edema model, the anti-edematous effect of CHD was further investigated in the three other standard models (histamine and serotonin induced paw volume and xylene induced ear edema). Histamine and serotonin can increase vascular permeability and both are effective vasodilators (Skidmore and Whitehouse, 1967) which are conducive to an ensuing edema. CHD not only suppressed the edema mediated by histamine and serotonin but also that of xylene at doses corresponding to standard anti-inflammatory drugs (Fig. 9A and B, 10A-B and 11). The xylene induced ear edema model is extensively utilized to determine the anti-inflammatory action of steroidal and non-steroidal anti-phlogistic agents (Zanini Jr et al., 1992). Studies reported in the literature have revealed that xylene also promotes vascular permeability causing skin edema owing to the release of inflammatory mediators leading to acute neurogenic inflammation (Bánki et al.,

2014). CHD markedly reduced ear edema induced by xylene comparable to the standard agents (Fig. 11).

To further corroborate the anti-nociceptive and anti-inflammatory potential of CHD, it was subjected to *in vitro* studies involving 5-LOX and COX-2 enzyme inhibition assays along with RT-PCR studies. Thus, CHD substantially inhibited 5-LOX and COX-2 enzymes in comparison with the standard inhibitors zileuton and celecoxib respectively as shown in (Table 2 and 3). In the case of RT-PCR studies, CHD decreased the mRNA expression of COX-2, TNF-α and IL-1β compared to the carrageenan treated control group as presented in Fig. 2. This *in vitro* study therefore endorsed the promising anti-nociceptive and anti-inflammatory findings with CHD in both the *in vivo* and *in silico* studies which further strengthens a potential for application in pain and inflammation.

In summary, *in silico* docking analysis demonstrated that the synthesized cyclohexanone derivative has shown favorable interactions with common pain targets i.e. COX 1/2, $GABA_A$ and opioid receptors (Figs. 12–14). The binding affinity study revealed that the intensity of interactions of the CHD ligand with the COX-2 isozyme was more than that with COX-1 and this was supported by the degree of 5-LOX and COX-2 enzyme inhibition observed (Table 2 and 3). In addition, MD simulations of the complexes revealed that CHD was a highly stable molecule at the docked site and generated robust chemical interactions underlying strong intermolecular affinity (Table 4). Interactions with other pharmacological targets suggest that CHD may act as a novel nociceptive and inflammatory pain reliever supported by *in vivo* studies (Figs. 3–11).

5. Conclusions

This study elucidated the synthesis and pharmacological evaluation of a novel cyclohexenone derivative (CHD) as a putative analgesic agent. CHD possessed not only anti-nociceptive, but also anti-inflammatory activity when tested in validated models of pain and inflammation in mice. These *in vivo* properties were attended by an inhibitory action on COX-2 and 5-LOX enzymes *in vitro* in addition to a complementary *in silico* interaction with $GABA_A$ and opioid receptors. Consequently, CHD represents an innovative and noteworthy anti-nociceptive and anti-inflammatory compound worthy of further pharmacological investigation and possible development.

Authors' contributions

GA conceived the research study and directed the research group as supervisor of the pharmacological experimentation. GA also interpreted the results in addition to critically reviewing the contents of the final version of manuscript. JK carried out the pharmacological experiments and performed the statistical analyses. He likewise developed the preliminary draft of the manuscript. RK helped in planning and supervising experiments related to the chemistry of our selected compound. UR conducted the computational studies and performed related calculations, interpretations and analysis. RU, MSJ, AAK, SA and SA helped in conducting the *in vitro* and *in silico* studies. All authors read and approved the final manuscript and RDES had an intellectual input in the writing of the manuscript and the interpretational outcome of the study.

CRediT authorship contribution statement

Jawad Khan: Methodology, Pharmacology, Investigation, Formal analysis, Writing – original draft, reading the final draft. **Gowhar Ali:** Conceptualization, Supervision, Writing – original draft, Writing – review & editing, preparation and reading the final draft. **Umer Rashid:** Methodology, Investigation, Formal analysis, Writing – original draft, Writing – review & editing, reading the final draft. **Rasool Khan:** Methodology, Supervision, Investigation. **Muhammad Saeed Jan:** Methodology, Investigation, Formal analysis, Writing – original draft, reading the final draft. **Rahim Ullah:** Methodology, Investigation, Formal analysis, Writing – original draft, reading the final draft. **Sajjad Ahmad:** Methodology, Investigation, Formal analysis, Writing – original draft, reading the final draft. **Sumra Wajid Abbasi:** Methodology, Investigation, Formal analysis, Writing – original draft, reading the final draft. **Atif Ali Khan Khalil:** Methodology, Investigation, Formal analysis, Writing – original draft, reading the final draft. **RobertD.E. Sewell:** Conceptualization, Writing – original draft, Writing – review & editing, preparation and reading the final draft.

Declaration of competing interest

The authors have no conflict of interest.

Acknowledgments

Dr. Umer Rashid is grateful to the Higher Education Commission of Pakistan for budgetary support for purchasing an MOE license under HEC-NRPU project 5291/Federal/NRPU/R&D/HEC/2016. The selected compound under study has been synthesized as a part of series of compounds with confirmed structures by Dr. Rasool Khan, Associate Professor, Institute of Chemical Science, University of Peshawar. We are grateful to him for providing a series of compounds and after preliminary study, we selected the cited compound (CHD) for our study.

References

Abbas, M., Subhan, F., Mohani, N., Rauf, K., Ali, G., Khan, M., 2011. The involvement of opioidergic mechanisms in the activity of Bacopa monnieriextract and its toxicological studies. Afr. J. Pharm. Pharmacol. 5, 1120–1124.

Abbasi, S., Raza, S., Azam, S.S., Liedl, K.R., Fuchs, J.E., 2016. Interaction mechanisms of a melatonergic inhibitor in the melatonin synthesis pathway. J. Mol. Liq. 221, 507–517.

Abro, A., Azam, S.S., 2016. Binding free energy based analysis of arsenic (+ 3 oxidation state) methyltransferase with S-adenosylmethionine. J. Mol. Liq. 220, 375–382.

Ahmad, N., Subhan, F., Islam, N.U., Shahid, M., Rahman, F.U., Sewell, R.D.J.E.j.o.p., 2017. Gabapentin and its salicylaldehyde derivative alleviate allodynia and hypoalgesia in a cisplatin-induced neuropathic pain model. Eur. J. Pharmacol. 814, 302–312.

Ahmadi, A., Khalili, M., Hajikhani, R., Hosseini, H., Afshin, N., Nahri-Niknafs, B., 2012. Synthesis and study the analgesic effects of new analogues of ketamine on female wistar rats. Med. Chem. 8, 246–251.

Akbar, S., Subhan, F., Karim, N., Shahid, M., Ahmad, N., Ali, G., Mahmood, W., Fawad, K.J.B., et al., 2016. 6-Methoxyflavanone attenuates mechanical allodynia and vulvodynia in the streptozotocin-induced diabetic neuropathic pain. Biomed. Pharmacother. 84, 962–971.

Ali, G., Subhan, F., Wadood, A., Ullah, N., Islam, N.U., Khan, I., 2013. Pharmacological evaluation, molecular docking and dynamics simulation studies of salicyl alcohol nitrogen containing derivatives. Afr. J. Pharm. Pharmacol. 7, 585–596.

Ali, G., Subhan, F., Abbas, M., Zeb, J., Shahid, M., Sewell, R.D., 2015. A streptozotocin-induced diabetic neuropathic pain model for static or dynamic mechanical allodynia and vulvodynia: validation using topical and systemic gabapentin. Naunyn-Schmiedeberg's Arch. Pharmacol. 388, 1129–1140.

Almeer, R.S., Hammad, S.F., Leheta, O.F., Abdel Moneim, A.E., Amin, H.K., 2019. Anti-inflammatory and anti-hyperuricemic functions of two synthetic hybrid drugs with dual biological active sites. Int. J. Mol. Sci. 20, 5635.

Amabeoku, G.J., Kabatende, J., 2012. Antinociceptive and anti-inflammatory activities of leaf methanol extract of Cotyledon orbiculata L.(Crassulaceae). Adv. Pharmacol. Sci 5–6.

Ayyad, S.-E.N., Judd, A.S., Shier, W.T., Hoye, T.R., 1998. Otteliones A and B: potently cytotoxic 4-methylene-2-cyclohexenones from Ottelia alismoides. J. Org. Chem. 63, 8102–8106.

Bánki, E., Hajna, Z., Kemeny, A., Botz, B., Nagy, P., Bolcskei, K., Tóth, G., Reglodi, D., Helyes, Z., 2014. The selective PAC1 receptor agonist maxadilan inhibits neurogenic vasodilation and edema formation in the mouse skin. Neuropharmacology 85, 538–547.

Bentley, G., Newton, S., Starr, J., 1983. Studies on the antinociceptive action of α-agonist drugs and their interactions with opioid mechanisms. Br. J. Pharmacol. 79, 125–134.

Burnett, B., Jia, Q., Zhao, Y., Levy, R., 2007. A medicinal extract of Scutellaria baicalensis and Acacia catechu acts as a dual inhibitor of cyclooxygenase and 5-lipoxygenase to reduce inflammation. J. Med. Food 10, 442–451.

Case, D., Darden, T., Cheatham III, T., Simmerling, C., Wang, J., Duke, R., Luo, R., Walker, R., Zhang, W., Merz, K., 2010. AMBER 12. There is no corresponding record for this reference.[Google Scholar]. University of California, San Francisco, pp. 1–826.

Chapman, C.R., Gavrin, J., 1999. Suffering: the contributions of persistent pain. Lancet 353, 2233–2237.

Chen, Y.-F., Tsai, H.-Y., Wu, T.-S., 1995. Anti-inflammatory and analgesic activities from roots of Angelica pubescens. Planta Med. 61, 2–8.
Cheon, M.S., Yoon, T., Choi, G., Moon, B.C., Lee, A.-Y., Choo, B.K., Kim, H.K., 2009. Chrysanthemum indicum Linné extract inhibits the inflammatory response by suppressing NF-κB and MAPKs activation in lipopolysaccharide-induced RAW 264.7 macrophages. J. Ethnopharmacol. 122, 473–477.
Danneman, P.J., Kiritsy-Roy, J.A., Morrow, T.J., Casey, K.L., 1994. Central delay of the laser-activated rat tail-flick reflex. Pain 58, 39–44.
Das, M., Manna, K., 2015. Bioactive cyclohexenones: a mini review. Curr. Bioact. Compd. 11, 239–248.
DiMasi, J.A., Feldman, L., Seckler, A., Wilson, A., 2010. Trends in risks associated with new drug development: success rates for investigational drugs. Clin. Pharmacol. Ther. 87, 272–277.
Duarte, I., Nakamura, M., Ferreira, S., 1988. Participation of the sympathetic system in acetic acid-induced writhing in mice. Braz. J. Med. Biol. Res. 21, 341–343.
Eddy, N.B., Leimbach, D., 1953. Synthetic analgesics. II. Dithienylbutenyl-and dithienylbutylamines. J. Pharmacol. Exp. Therapeut. 107, 385–393.
Fang, S.-M., Cui, C.-B., Li, C.-W., Wu, C.-J., Zhang, Z.-J., Li, L., Huang, X.-J., Ye, W.-C., 2012. Purpurogemutantin and purpurogemutantidin, new drimenyl cyclohexenone derivatives produced by a mutant obtained by diethyl sulfate mutagenesis of a marine-derived Penicillium purpurogenum G59. Mar. Drugs 10, 1266–1287.
Fawad, K., Islam, N.U., Subhan, F., Shahid, M., Ali, G., Rahman, F.-U., Mahmood, W., Ahmad, N., 2018. Novel hydroquinone derivatives alleviate algesia, inflammation and pyrexia in the absence of gastric ulcerogenicity. Trop. J. Pharmaceut. Res. 17, 53–63.
Fernandes, J.V., Cobucci, R.N.O., Jatobá, C.A.N., de Medeiros Fernandes, T.A.A., de Azevedo, J.W.V., de Araújo, J.M.G., 2015. The role of the mediators of inflammation in cancer development. Pathol. Oncol. Res. 21, 527–534.
Gopalakrishnan, M., Thanusu, J., Kanagarajan, V., 2008. Synthesis and characterization of 4, 6-diaryl-4, 5-dihydro-2H-indazol-3-ols and 4, 6-diaryl-2-phenyl-4, 5-dihydro-2H-indazol-3-ols—a new series of fused indazole derivatives. Chem. Heterocycl. Compd. 44, 950–955.
Gutthann, S.P., Rodríguez, L.A.G., Raiford, D.S., Oliart, A.D., Romeu, J.R., 1996. Nonsteroidal anti-inflammatory drugs and the risk of hospitalization for acute renal failure. Arch. Intern. Med. 156, 2433–2439.
Hunskaar, S., Hole, K., 1987. The formalin test in mice: dissociation between inflammatory and non-inflammatory pain. Pain 30, 103–114.
Iftikhar, F., Ali, Y., Kiani, F.A., Hassan, S.F., Fatima, T., Khan, A., Niaz, B., Hassan, A., Ansari, F.L., Rashid, U., 2017. Design, synthesis, in vitro Evaluation and docking studies on dihydropyrimidine-based urease inhibitors. Bioorg. Chem. 74, 53–65.
Iftikhar, F., Yoqoob, F., Tabassum, N., Jan, M.S., Sadiq, A., Tahir, S., Batool, T., Niaz, B., Ansari, F.L., Chaudhary, M.I., 2018. Design, synthesis, in-vitro thymidine phosphorylase inhibition, in-vivo antiangiogenic and in-silico studies of C-6 substituted dihydropyrimidines. Bioorg. Chem. 80, 99–111.
Islam, N.U., Amin, R., Shahid, M., Amin, M., Zaib, S., Iqbal, J., 2017. A multi-target therapeutic potential of Prunus domestica gum stabilized nanoparticles exhibited prospective anticancer, antibacterial, urease-inhibition, anti-inflammatory and analgesic properties. BMC Compl. Alternative Med. 17, 272–276.
Islam, N.U., Jalil, K., Shahid, M., Rauf, A., Muhammad, N., Khan, A., Shah, M.R., Khan, M.A., 2019. Green synthesis and biological activities of gold nanoparticles functionalized with Salix alba. Arab. J. Chem. 12, 2914–2925.
Jan, M.S., Ahmad, S., Hussain, F., Ahmad, A., Mahmood, F., Rashid, U., Ullah, F., Ayaz, M., Sadiq, A.J.E.j.o.m.c., 2020. Design, synthesis, in-vitro, in-vivo and in-silico studies of pyrrolidine-2, 5-dione derivatives as multitarget anti-inflammatory agents. Eur. J. Med. Chem. 186, 111863.
Johnson, T., Pultar, F., Menke, F., Lautens, M., 2016. Palladium-catalyzed α-arylation of vinylogous esters for the synthesis of γ, γ-disubstituted cyclohexenones. Org. Lett. 18, 6488–6491.
Jones, R., Rubin, G., Berenbaum, F., Scheiman, J., 2008. Gastrointestinal and cardiovascular risks of nonsteroidal anti-inflammatory drugs. Am. J. Med. 121, 464–474.
Kanagarajan, V., Ezhilarasi, M., Bhakiaraj, D., Gopalakrishnan, M., 2013. In vitro anticandidal evaluation of novel highly functionalized bis cyclohexenone ethyl carboxylates. Eur. Rev. Med. Pharmacol. Sci. 17, 292–298.
Khalid, S., Ullah, M.Z., Khan, A.U., Afridi, R., Rasheed, H., Khan, A., Ali, H., Kim, Y.S., Khan, S., 2018. Antihyperalgesic properties of honokiol in inflammatory pain models by targeting of NF-κB and Nrf2 signaling. Front. Pharmacol. 9, 140.
Khan, J., Ali, G., Khan, R., Ullah, R., Ullah, S., 2019. Attenuation of vincristine-induced neuropathy by synthetic cyclohexenone-functionalized derivative in mice model. Neurol. Sci. 1–13.
Kidd, B., Urban, L., 2001. Mechanisms of inflammatory pain. Br. J. Anaesth. 87, 3–11.
Laxmaiah Manchikanti, M., Bert Fellows, M., Hary Ailinani, M., 2010. Therapeutic use, abuse, and nonmedical use of opioids: a ten-year perspective. Pain. Physician 13, 401–435.
Lednicer, D., Von Voigtlander, P.F., Emmert, D.E., 1981a. 4-Aryl-4-aminocyclohexanones and their derivatives, a novel class of analgesics. 3. m-hydroxyphenyl derivatives. J. Med. Chem. 24, 341–346.
Lednicer, D., VonVoigtlander, P.F., Emmert, D.E., 1981b. 4-Amino-4-arylcyclohexanones and their derivatives: a novel class of analgesics. 2. Modification of the carbonyl function. J. Med. Chem. 24, 404–408.
Ledoux, A., St-Gelais, A., Cieckiewicz, E., Jansen, O., Bordignon, A., Illien, B., Di Giovanni, N., Marvilliers, A., Hoareau, F., Pendeville, H., 2017. Antimalarial activities of alkyl cyclohexenone derivatives isolated from the leaves of Poupartia borbonica. J. Nat. Prod. 80, 1750–1757.
Liu, D., Yu, W., Li, J., Pang, C., Zhao, L., 2013. Novel 2-(E)-substituted benzylidene-6-(N-substituted aminomethyl) cyclohexanones and cyclohexanols as analgesic and anti-inflammatory agents. Med. Chem. Res. 22, 3779–3786.
Malan, T.P., Mata, H.P., Porreca, F., 2002. Spinal GABAAand GABABReceptor pharmacology in a rat model of neuropathic pain. Anesthesiology 96, 1161–1167.
Manouze, H., Bouchatta, O., Gadhi, A.C., Bennis, M., Sokar, Z., Ba-M'hamed, S., 2017. Anti-inflammatory, antinociceptive, and antioxidant activities of methanol and aqueous extracts of Anacyclus pyrethrum roots. Front. Pharmacol. 8, 592–598.
Masresha, B., Makonnen, E., Debella, A., 2012. In vivo anti-inflammatory activities of Ocimum suave in mice. J. Ethnopharmacol. 142, 201–205.
Mayer, D.J., Mao, J., Price, D.D., 1995. The development of morphine tolerance and dependence is associated with translocation of protein kinase C. Pain 61, 365–374.
Mazzanti, G., Braghiroli, L., 1994. Analgesic antiinflammatory action of Pfaffia paniculata (Martius) kuntze. Phytother Res. 8, 413–416.
McCarson, K.E., Enna, S., 2014. GABA pharmacology: the search for analgesics. Neurochem. Res. 39, 1948–1963.
Mequanint, W., Makonnen, E., Urga, K., 2011. In vivo anti-inflammatory activities of leaf extracts of Ocimum lamiifolium in mice model. J. Ethnopharmacol. 134, 32–36.
Miller III, B.R., McGee Jr., T.D., Swails, J.M., Homeyer, N., Gohlke, H., Roitberg, A.E., 2012. MMPBSA. py: an efficient program for end-state free energy calculations. J. Chem. Theor. Comput. 8, 3314–3321.
Ming-Tatt, L., Khalivulla, S.I., Akhtar, M.N., Lajis, N., Perimal, E.K., Akira, A., Ali, D.I., Sulaiman, M.R., 2013. Anti-Hyperalgesic effect of a benzilidine-cyclohexanone analogue on a mouse model of chronic constriction injury-induced neuropathic pain: participation of the κ-Opioid receptor and KATP. Pharmacol. Biochem. Behav. 114, 58–63.
Ming-Tatt, L., Khalivulla, S.I., Akhtar, M.N., Mohamad, A.S., Perimal, E.K., Khalid, M.H., Akira, A., Lajis, N., Israf, D.A., Sulaiman, M.R., 2012. Antinociceptive activity of a synthetic curcuminoid analogue, 2, 6-bis-(4-hydroxy-3-methoxybenzylidene) cyclohexanone, on nociception-induced models in mice. Basic Clin. Pharmacol. Toxicol. 110, 275–282.
Monga, V., Goyal, K., Steindel, M., Malhotra, M., Rajani, D.P., Rajani, S.D., 2014. Synthesis and evaluation of new chalcones, derived pyrazoline and cyclohexenone derivatives as potent antimicrobial, antitubercular and antileishmanial agents. Med. Chem. Res. 23, 2019–2032.
Mousavi, S.R., 2016. Claisen–Schmidt condensation: synthesis of (1S, 6R)/(1R, 6S)-2-oxo-N, 4, 6-triarylcyclohex-3-enecarboxamide derivatives with different substituents in H2O/EtOH. Chirality 28, 728–736.
Muhammad, N., Saeed, M., Khan, H., 2012. Antipyretic, analgesic and anti-inflammatory activity of Viola betonicifolia whole plant. BMC Compl. Alternative Med. 12, 53–59.
Nazar, M.F., Abdullah, M.I., Badshah, A., Mahmood, A., Rana, U.A., Khan, S.U.-D., 2015. Synthesis, structure–activity relationship and molecular docking of cyclohexenone based analogous as potent non-nucleoside reverse-transcriptase inhibitors. J. Mol. Struct. 1086, 8–16.
Okoth, D.A., Koorbanally, N.A., 2015. Cardanols, long chain cyclohexenones and cyclohexenols from Lannea schimperi (Anacardiaceae). Nat. Prod. Commun. 10, 103–106.
Okoth, D.A., Akala, H.M., Johnson, J.D., Koorbanally, N.A., 2016. Alkyl phenols, alkenyl cyclohexenones and other phytochemical constituents from Lannea rivae (chiov) Sacleux (Anacardiaceae) and their bioactivity. Med. Chem. Res. 25, 690–703.
Olonode, E.T., Aderibigbe, A.O., Bakre, A.G., 2015. Anti-nociceptive activity of the crude extract of Myrianthus arboreus P. Beauv (Cecropiaceae) in mice. J. Ethnopharmacol. 171, 94–98.
Patel, S., Naeem, S., Kesingland, A., Froestl, W., Capogna, M., Urban, L., Fox, A., 2001. The effects of GABAB agonists and gabapentin on mechanical hyperalgesia in models of neuropathic and inflammatory pain in the rat. Pain 90, 217–226.
Pini, L.A., Vitale, G., Ottani, A., Sandrini, M., 1997. Naloxone-reversible antinociception by paracetamol in the rat. J. Pharmacol. Exp. Therapeut. 280, 934–940.
Rashid, U., Sultana, R., Shaheen, N., Hassan, S.F., Yaqoob, F., Ahmad, M.J., Iftikhar, F., Sultana, N., Asghar, S., Yasinzai, M., 2016. Structure based medicinal chemistry-driven strategy to design substituted dihydropyrimidines as potential antileishmanial agents. Eur. J. Med. Chem. 115, 230–244.
Rodrigues, M.R.A., Kanazawa, L.K.S., das Neves, T.L.M., da Silva, C.F., Horst, H., Pizzolatti, M.G., Santos, A.R.S., Baggio, C.H., de Paula Werner, M.F., 2012. Antinociceptive and anti-inflammatory potential of extract and isolated compounds from the leaves of Salvia officinalis in mice. J. Ethnopharmacol. 139, 519–526.
Rukh, L., Ali, G., Ullah, R., Islam, N.U., Shahid, M.J.E.J.o.P., 2020. Efficacy assessment of salicylidene salicylhydrazide in chemotherapy associated peripheral neuropathy. Eur. J. Pharmacol. 888, 173481.
Said, S.A., Amr, A.E.-G.E., Sabry, N.M., Abdalla, M.M., 2009. Analgesic, anticonvulsant and anti-inflammatory activities of some synthesized benzodiazipine, triazolopyrimidine and bis-imide derivatives. Eur. J. Med. Chem. 44, 4787–4792.
Salinas-Abarca, A.B., Avila-Rojas, S.H., Barragán-Iglesias, P., Pineda-Farias, J.B., Granados-Soto, V.J.E.j.o.p., 2017. Formalin injection produces long-lasting hypersensitivity with characteristics of neuropathic pain. Eur. J. Pharmacol. 797, 83–93.
Saranya, A.V., Ravi, S., 2012. Synthesis, characterization and anti-bacterial activity of pyrimidine, cyclohexenone and 1, 5-diketone derivatives of furfural chalcone. J. Pharm. Res. 5, 1098–1101.
Sawynok, J., 1984. GABAergic mechanisms in antinociception. Prog. Neuro-Psychopharmacol. Biol. Psychiatry 8, 581–586.
Senguttuvan, S., Nagarajan, S., 2010. Synthesis of 2-amino-5-aryl-5, 6-dihydro-7-(naphthalen-2-yl) quinazolin-4-ols. Int. J. Chem. 2, 108.
Sewell, R., Spencer, P., 1976. Antinociceptive activity of narcotic agonist and partial agonist analgesics and other agents in the tail-immersion test in mice and rats. Neuropharmacology 15, 683–688.

Shahid, M., Subhan, F., Ullah, I., Ali, G., Alam, J., Shah, R., 2016. Beneficial effects of Bacopa monnieri extract on opioid induced toxicity. Heliyon 2, e00068.
Shahid, M., Subhan, F., Ahmad, N., Ali, G., Akbar, S., Fawad, K., Sewell, R., 2017a. Topical gabapentin gel alleviates allodynia and hyperalgesia in the chronic sciatic nerve constriction injury neuropathic pain model. Eur. J. Pain 21, 668–680.
Shahid, M., Subhan, F., Ahmad, N., Ullah, I., 2017b. A bacosides containing Bacopa monnieri extract alleviates allodynia and hyperalgesia in the chronic constriction injury model of neuropathic pain in rats. BMC Compl. Alternative Med. 17, 293.
Sheorey, R., Thangathiruppathy, A., Alagarsamy, V., 2016. Synthesis and pharmacological evaluation of 3-propyl-2-substitutedamino-3H-quinazolin-4-ones as analgesic and anti-inflammatory agents. J. Heterocycl. Chem. 53, 1371–1377.
Silva, R.H., Lima, N.d.F.M., Lopes, A.J., Vasconcelos, C.C., de Mesquita, J.W., de Mesquita, L.S., Lima, F.C., Ribeiro, M.N.d.S., Ramos, R.M., Cartágenes, M.d.S.d.S., 2017. Antinociceptive activity of borreria verticillata: in vivo and in silico studies. Front. Pharmacol. 8, 283.
Skidmore, I., Whitehouse, M., 1967. Biochemical properties of anti-inflammatory drugs—X: the inhibition of serotonin formation in vitro and inhibition of the esterase activity of α-chymyotrypsin. Biochem. Pharmacol. 16, 737–751.
Suba, V., Murugesan, T., Kumaravelrajan, R., Mandal, S.C., Saha, B., 2005. Antiinflammatory, analgesic and antiperoxidative efficacy of Barleria lupulina Lindl. extract. Phytother. Res. 19, 695–699.
Systemes, D., 2015. BIOVIA, Discovery Studio Modeling Environment. Release 4.5. Dassault Systemes, San Diego, CA.
Tjølsen, A., Berge, O.-G., Hunskaar, S., Rosland, J.H., Hole, K., 1992. The formalin test: an evaluation of the method. Pain 51, 5–17.
Ullah, R., Ali, G., Subhan, F., Naveed, M., Khan, A., Khan, J., Halim, S.A., Ahmad, N., Al-Harrasi, A., 2021. Attenuation of nociceptive and paclitaxel-induced neuropathic pain by targeting inflammatory, CGRP and substance P signaling using 3-Hydroxyflavone. Neurochem. Int. 144, 104981.
Utsunomiya, I., Ito, M., Oh-ishi, S., 1998. Generation of inflammatory cytokines in zymosan-induced pleurisy in rats: TNF induces IL-6 and cytokine-induced neutrophil chemoattractant (CINC) in vivo. Cytokine 10, 956–963.
Van Hecke, O., Austin, S.K., Khan, R.A., Smith, B., Torrance, N., 2014. Neuropathic pain in the general population: a systematic review of epidemiological studies. Pain 155, 654–662.
Wang, Y., Yu, C., Pan, Y., Li, J., Zhang, Y., Ye, F., Yang, S., Zhang, H., Li, X., Liang, G., 2011. A novel compound C12 inhibits inflammatory cytokine production and protects from inflammatory injury in vivo. PloS One 6, e24377.
Wisastra, R., Kok, P.A., Eleftheriadis, N., Baumgartner, M.P., Camacho, C.J., Haisma, H. J., Dekker, F.J., 2013. Discovery of a novel activator of 5-lipoxygenase from an anacardic acid derived compound collection. Bioorg. Med. Chem. 21, 7763–7778.
Yaouba, S., Koch, A., Guantai, E.M., Derese, S., Irungu, B., Heydenreich, M., Yenesew, A., 2018. Alkenyl cyclohexanone derivatives from Lannea rivae and Lannea schweinfurthii. Phytochem. Lett. 23, 141–148.
Zanini Jr., J.C., Medeiros, Y.S., Cruz, A.B., Yunes, R.R., Calixto, J.B., 1992. Action of compounds from Mandevilla velutina on croton oil-induced ear oedema in mice. A comparative study with steroidal and nonsteroidal antiinflammatory drugs. Phytother Res. 6, 1–5.
Maione, F., Colucci, M., Raucci, F., Mangano, G., Marzoli, F., Mascolo, N., Crocetti, L., Giovannoni, M.P., Di Giannuario, A., Pieretti, S., 2020. New insights on the arylpiperazinylalkyl pyridazinone ET1 as potent antinociceptive and anti-inflammatory agent. Eur. J. Pharmacol., 173572